ISSN 1062-7391, Journal of Mining Science, 2018, Vol. 54, No. 2, pp. 270–284. © Pleiades Publishing, Ltd., 2018.
Published in Fiziko-Tekhnicheskie Problemy Razrabotki Poleznykh Iskopaemykh, 2018, No. 2, pp. 98–113.

MINERAL MINING TECHNOLOGY

Penetration Rate and Specific Energy Prediction of Rotary–Percussive Drills Using Drill Cuttings and Engineering Properties of Selected Rock Units

M. Z. Abu Bakar[a]*, I. A. Butt[b], and Y. Majeed[c]

[a]Geological Engineering Department, University of Engineering and Technology, Lahore, Pakistan
[b]Department of Civil Engineering, University of Lahore, Lahore, Pakistan
*e-mail: mzubairab1977@gmail.com
[c]Mining Engineering Department, University of Engineering and Technology, Lahore, Pakistan

Received February 15, 2017

Abstract—This study discusses the prediction of penetration rate and specific energy of button bit equipped rotary–percussion drilling machines from drill cuttings and geo-mechanical properties of rocks. The operational parameters of drilling machines measured from selected locations were utilized for the calculation of specific energy of drilling operations. For this purpose three on-going hydropower projects and four active mining quarries of Pakistan were selected. The drill cuttings were further used to determine various descriptors of the chip size distribution including the coarseness index and Rosin–Rammler's absolute size constant. A complete set of geo-mechanical rock tests were conducted in the laboratory and includes uniaxial compressive strength, Brazilian tensile strength, point load strength, Schmidt rebound hardness, *P*-wave velocity, dry density, porosity and brittleness indices. Regression analyses were performed to predict the penetration rate and specific energy of drilling from geo-mechanical properties of rocks. The models so developed were also validated by adopting the *t*-test and the *F*-test statistical techniques. Moreover, statistical models were also developed to evaluate penetration rate from various descriptors of the chip size distribution. Dependence of bit size on coarseness index and mean particle size was also discussed.

Keywords: Penetration rate, specific energy, coarseness index, Rosin–Rammler's constant, uniaxial compressive strength, Brazilian tensile strength, point load strength, Schmidt rebound hardness, density, porosity, *P*-wave velocity.

DOI: 10.1134/S106273911802363X

INTRODUCTION

In Pakistan various types of underground excavations including highway tunnels, pressure tunnels, hydropower caverns, railway tunnels amongst others, are being driven by the drilling and blasting technique due to its versatility, flexibility, economics and low initial capital cost. The drill and blast is considered to be a suitable technique of excavation in almost every ground condition encountered during surface and underground excavations. However, as reported by McFeat-Smith and Fowell [1] the cost of drill and blast technique increases as the excavation length exceeds more than 1.5–2.0 km. Although, the advance rate of mechanical excavators is approximately 40% better than the drill and blast technique, but due to sudden variations of underground field conditions which cannot be assessed during site investigation, sometimes makes mechanical excavation inflexible and limited.

The efficiency of any drilling operation is usually measured in terms of its penetration rate and specific energy consumed to achieve that penetration rate. Penetration rate or drillability is defined as the time required for drilling a unit depth of rock. It has been widely used for rock classification in mining industry [2]. It is usually determined by a set of parameters including geo-mechanical properties of rocks (uncontrollable parameters) and drilling machine parameters (rotation, thrust force, flushing, etc.). Operating process (drilling method, operation and maintenance of machine) also plays a vital role in the drillability of rocks. Both drilling machine parameters and operating process are considered to be controllable parameters in drilling of rocks [3].

Performance prediction (penetration rate) of the percussive/rotary drills as well as tunnel boring machines (TBMs), road headers and raise borers by using size distribution of the drill cuttings through coarseness index (CI), mean particle size (absolute size constant D') and median size constant d has been investigated by a number of researchers. Pfleider and Blake [4] reported the existence of a rough relationship between the size range of drill cuttings and the penetration rate. Rabia and Brook [5] compared the surface area of drill cutting with the penetration rate of down the hole drill (DTH) and found that no relationship exists between surface area of drill cutting and penetration rate of drill. Ersoy and Waller [6] concluded that wear rate of bits depend upon the size of drill cuttings; larger size of drill cuttings cause rapid wear in impregnated diamond core drilling bits, thereby reducing the penetration rate. Altindag [3, 7] explored a strong exponential relationship between penetration rate and coarseness index. Meanwhile by using Rosin–Rammler plot the cited author also found exponential relationships of penetration rate with mean particle size (absolute size constant D') and specific surface area of drill cuttings. Kahraman et al. [8] proposed strong linear correlations of penetration rate with coarseness index and median particle size of drill cuttings. Similarly, Tuncdemir et al. [9] calculated the in situ coarseness index values of muck size collected for different cutting depths per revolution of TBM and found a linear relationship between coarseness index and advance rate per revolution. Abu Bakar and Gertsch [10] reported a good relationship between coarseness index and the absolute chip size constant in a full scale rock cutting test. In a similar study, Abu Bakar et al. [11] examined reasonable relationships of absolute size constant and coarseness index with production rate (advance rate) of constant cross section (CCS) disc cutter.

Geo-mechanical properties of rocks are good indicators of penetration rate and a number of previous investigators have established relationships showing dependence of penetration rate on rock properties. Selmer-Olsen and Blindheim [12] while performing percussion drilling tests in the field established that some rock properties (e.g. UCS and BTS) strongly influence the drilling operation. Howarth et al. [13] monitored the performance of TBM and diamond bit percussion drilling machines and figured out meaningful relationships of penetration rate with some physico-mechanical properties of sedimentary rocks. They also highlighted that rock porosity directly influences drillability. Thuro and Spaun [14] while measuring the drilling rates of two machines (15 kW and 20 kW) found logarithmic relationships of penetration rate with the compressive and tensile strengths. Thuro [15] demonstrated that some specific rock properties and geological factors significantly influence the bit wear and drilling rate. Altindag [16] proposed a correlation between the rock brittleness and drillability index and highlighted that brittleness causes an increase in the penetration rate. Kahraman et al. [17] developed significant correlations of penetration rate of percussive drills with UCS, BTS, PLS and SRH of rocks. Dahl et al. [18] performed a comparative study of different test methods utilized for the prediction of drillability on a laboratory scale and presented tables for the selection of a reliable drilling bit based on rock properties. Seifabad and Ehteshami [19] suggested empirical equations for the estimation of drilling rates based on models derived from rock properties of 50 oil wells. Ngerebara et al. [20] correlated the mechanical properties of some rocks with the penetration rate of rotary drilling rig. Similarly, the drilling rate of pneumatic top hammer drills was related with dry density, UCS, BTS, SRH and Young's modulus of nine rocks by Hoseinie et al. [21].

Specific energy (SE) is defined as the energy required to fragment a unit volume of rock [22–25]. According to Rabia [26], it is the energy to create a new surface area. Bullock [27] investigated some drilling systems including rotary drills, percussive drills and rotary-percussive drills in Bonneterre

Dolomite and found an inverse relationship between the chip size and specific energy of drilling. It is well known from work of some previous researchers [10, 28, 29,] that specific energy in rock cutting is affected significantly by tool geometry, cutter spacing, tool penetration and rock properties. However, in rotary drilling or in rock cutting using drag tools, tensile strength, compressive strength and shear strength are the dominant rock properties affecting the cutting efficiency [30, 31]. Copur et al. [25] performed full-scale laboratory rock-cutting tests with a conical cutter and explained that optimum specific energy is a direct function of rock parameters (UCS and BTS). Altindag [3] correlated specific energy of rock cutting with three brittleness indices $B_1 = \sigma_c / \sigma_t$, $B_2 = (\sigma_c - \sigma_t)/(\sigma_c + \sigma_t)$ and $B_3 = (\sigma_c \sigma_t)/2$, where $\sigma_c = \text{UCS}$ and $\sigma_t = \text{BTS}$. Similarly, Atici and Ersoy [32] statistically evaluated the relationships between brittleness and cutting specific energy of diamond saw blades and drilling specific energy of polycrystalline diamond compact (PDC) bits. Good correlations were found between brittleness indices (B_1, B_2 and B_3) and cutting specific energy whereas no reasonable correlations were found between the drilling specific energy and the brittleness values.

At present button bits employed in rotary-percussive drilling rigs are commonly being used in almost every rock drilling project, but their drillability rates are not properly documented in different rock formations of Pakistan. There is a need of penetration prediction models based on the geo-mechanical properties of rocks, chip size distribution of drill cuttings and drilling machine's operational parameters. In this study, a number of parameters including, the actual penetration rate of button bits measured in the field, coarseness index CI, the Rosin–Rammler's absolute size constant D', specific energy of drilling, brittleness indices and geo-mechanical properties are determined on rock units encountered in selected ongoing tunneling and mining projects of Pakistan. The results obtained would be of significant import for the contractors involved in the current and future mega projects such as dams, tunnels, highways and the foundations for mega structures in Pakistan.

1. RESEARCH METHODOLOGY

The research methodology is mainly comprised of field studies and laboratory studies along with calculation of specific energy of drilling.

1.1. Field Work

Field work was conducted on nine different rock types selected from seven on-going tunneling and mining projects (Fig. 1) in Pakistan. Table 1 lists the selected projects along with their formations and geological age. The field work included recording of drilling parameters, collection of drill cuttings from the boreholes and selection of representative rock blocks from the working sites.

1 — GHPP (Gulpure Hydropower project AJK)
2 — NJHPP (Neelum Jhelum Hydroelectric Project AJK)
3 — KHPP (Karora Hydropower Project KPK)
4 — DGKCCL (D, G, Khan Cement Company Limited Punjab)
5 — KCCL (Kohat Cement Company Limited KPK)
6 — GCC (Gharibwal Cement Limited Punjab)
7 — MLCFL (Maple Leat Cement Factory Limited Punjab)

Fig. 1. Included project locations marked on the map of Pakistan.

Table 1. Selected projects along with their locations and rock types

No.	Project	Location	Rock type	Formation / Group	Geological Age
1	GHPP	Kotli, Azad Kashmir, Pakistan	Nagri Sandstone	Nagri	Miocene
2	NJHPP	Muzaffarabad Azad Jamu and Kashmir (AJK), Pakistan	Murree Sandstone	Murree	Miocene
3	KHPP	Besham, Shangla, Khyber Pakhtunkhwa (KPK), Pakistan	Granitic Gneiss	Besham Group	Precambrian
4	KHPP	Besham, Shangla, Khyber Pakhtunkhwa (KPK), Pakistan	Graphitic Gneiss	Besham Group	Precambrian
5	DGKCCL	Khofli Sattai, D.G. Khan, Punjab Pakistan	Dungan Limestone	Dungan Limestone	Cretaceous
6	KCCL	Kohat, Khyber Pakhtunkhwa (KPK), Pakistan	Lockhart Limestone	Lockhart Limestone	Paleocene
7	KCCL	Kohat, Khyber Pakhtunkhwa (KPK), Pakistan	Dolomite	Smana Suk	Jurassic
8	GCL	Ismailwal, Chakwal, Punjab, Pakistan	Sakesar limestone	Sakesar Limestone	Eocene
9	MLCFL	Iskanderabad, Mianwali, Punjab, Pakistan	Nammal Limestone	Nammal	Eocene

GHPP—Gulpur Hydropower project; NJHPP—Neelum Jhelum Hydroelectric Project; KHPP—Karora Hydropower Project; DGKCCL—D.G. Khan Cement Company Limited; KCCL—Kohat Cement Company Limited; GCL—Gharibwal Cement Limited; MLCFL—Maple Leaf Cement Factory Limited

1.1.1. Recording of drilling parameters in the field

Button bit employed in rotary-percussive rock drills were utilized on selected mega hydropower projects and cement quarries. Figure 2 shows a view of drilling operation carried out for rock bolting at NJHPP in Murree Sandstone rock unit with the help of Sandvick Power Pack HP555, hydraulic drill. A description of rock drills, bit sizes, rotational speeds and working pressures employed on respective locations is provided in Table 2. The rock drills were controlled by the drilling operators according to the rock conditions encountered at the working faces. The operating parameters such as feed pressure, rotational pressure, working pressure and flushing pressure were recorded while boreholes were being drilled. In addition, the rotational speed and torque were also recorded from the catalogs of respective rotary-percussive drills. In each project on the average 25 bore holes were drilled on each drilling day for blasting as well as for rock bolt installation purposes. Actual drilling time of 7 to 12 boreholes in each selected rock unit was recorded and the corresponding boreholes depths were measured accurately. The borehole diameter and the bit diameter were also measured. The borehole depth and drilling time measured for each borehole in each selected rock unit was further used to calculate the penetration rate by using equation.

$$\text{PR} = \text{Depth of borehole, m / Drilling time, мin}\,. \quad (1)$$

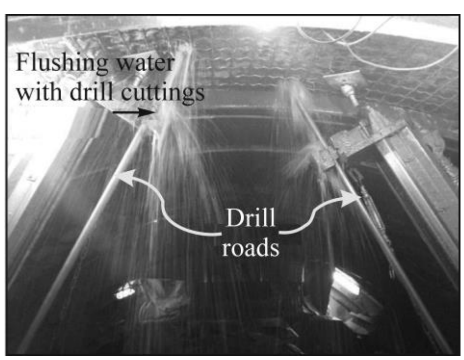

Fig. 2. A view of Sandvick Power Pack HP555, hydraulic rotary percussive drill machine working at NJHPP.

Table 2. Summary of rotary percussive rock drills being used on seven selected projects

Project	Rock Drill (Rotary-Percussion Type)	Button Bit Diameter, mm	Ratational Speed, rpm	Working Pressure, kPa
KHPP	Atlas Copco XAS 186DD (pneumatic top hammer)	34	250.2	610
NJHPP	Sandvick Power Pack HP555 (hydraulic rock bolt drill)	48	250.2	800
GHPP	Furukawa HCR180 (hydraulic top hammer)	65	130.2	650
KCCL	Furukawa HCR C180R (hydraulic top hammer)	75	120.0	600
MLCFL	Ingersoll Rand–LM500 (hydraulic top hammer)	85	90.0	650
GCL	MP-CMP-0002 (pneumatic top hammer)	105	60.0	840
DGKCCL	Atlas Copco ROC L6 (DTH)	105	70.2	850

The average actual field penetration rate of 7–12 boreholes in each selected rock unit was then calculated and further utilized for analysis.

The specific energy (SE) of drilling was also calculated for each selected rock from the measured drilling parameters of rock drills by using the following equation [23]:

$$\mathrm{SE}=\mathrm{SE}_\mathrm{t}+\mathrm{SE}_\mathrm{r}, \quad \mathrm{SE}_\mathrm{t}=F/A, \quad \mathrm{SE}_\mathrm{r}=(2\pi/A)/(NT/\mathrm{PR}), \tag{2}$$

where SE is specific energy, MJ/m^3; SE_t is specific energy due to thrust, MJ/m^3; SE_r is specific energy due to rotation, MJ/m^3; F is force acting on the bit, kN; A is borehole cross sectional area, m^2; N is rotational speed, rev/s; T is torque (KNm) and PR is penetration rate (m/s).

1.1.2. Collection of borehole drill cuttings and selection of rock boulders

The drill cuttings from selected boreholes of each rock unit were collected in polythene bags and labeled carefully. To prevent possible error of removing label from bags, the drills cuttings were further stored in plastic jars in the laboratory. In addition to this, the rock blocks of selected rock unit were collected from the same field for further laboratory studies. Blocks free from micro and macro discontinuities were selected in appropriate dimensions in order to retrieve maximum number of cores for conducting physical and mechanical properties tests in the laboratory.

1.2. Laboratory Studies

A comprehensive suite of laboratory experiments comprising of sieve analysis of drill cuttings collected from the drilling sites, rock mechanics tests including UCS, BTS, PLS and SRH, density, porosity and sonic velocity tests were performed. For performing mechanical and physical rock properties tests, cores were retrieved from the collected blocks orthogonal to the bedding by using 54 mm core cutting bits. The cylindrical rock specimens were prepared according to the guidelines laid down in ASTM-D4543 [36] standards.

1.2.1. Sieve analysis on drill cuttings

The correlation between performance of drilling systems and distribution of drill cuttings can be described with the help of coarseness index CI and the absolute size constant D'. Parameters like coarseness index and the absolute size constant D' have been used by past investigators [3, 8, 10, 11, 37] to evaluate the performance of different rock cutting and drilling systems. CI is a dimensionless number which is obtained from the cumulative sum of percentage size retained (oversize) of drill cuttings on particular selected sieve fractions. The range of coarseness index depends on a particular set of sieve used [37].

Table 3. The extraction of coarseness index from drill cuttings (borehole no. 1) against bit diameter of 75 mm in Lockhart limestone

Sieve Fraction, mm	Weight Oversize, g	Weight Oversize, %	Cumulative Oversize, %
+19.00	0	0	0
−19.00+9.51	60	1.65	1.65
−9.51+4.76	134	3.68	5.33
−4.76+2.00	1202	33.05	38.38
−2.00+1.00	794	21.83	60.21
−1.00+0.50	532	14.63	74.84
−0.50+0.25	592	16.28	91.12
Pan	323	8.88	100.00
Total Mass	3637	—	CI = 372

The absolute size constant D' of particle distribution can be determined by adopting the Rosin–Rammler [38] method; also used frequently to evaluate the products of tumbling mills in the mineral processing industry. The Rosin–Rammler distribution describes the mass (volume) distribution function in exponential form as:

$$R = 100\exp[-(x / D')^{b}], \tag{3}$$

where R is the cumulative mass (volume) % retained on sieve of size x; D' is the absolute size constant or size parameter, and b is the distribution parameter.

Rearranging and taking logarithm twice of both sides of equation 3 gives:

$$\ln[\ln(100 / R)] = b\ln x + \text{const}. \tag{4}$$

The values of $\log[\log(100/R)]$ when plotted against $\log x$ gives a straight line. The slope of this straight line and the intercept at the horizontal line at $R = 36.79\%$ provides the Rosin–Rammler distribution parameters b and D' respectively. Both of these parameters completely define the particle size distribution.

In the current research work the drill cuttings of 7–12 boreholes of each nine selected rock units were sieved by using seven sieve fractions (i.e. +19 mm, +9.51, +4.76, +2, +1, +0.5, and +0.25 mm) to determine CI value. Table 3 displays a sample calculation of CI for Lockhart limestone. Similarly, the absolute size constant D' was calculated by employing the Rosin–Rammler plot between sieve opening and cumulative weight (%) as explained by Aytekin [39]. Figure 3 is the Rosin–Rammler graph plotted by using the data displayed in Table 4 and shows the determination of D' and b for the drill cuttings gathered from borehole no. 1 of same rock (Lockhart limestone) as an example.

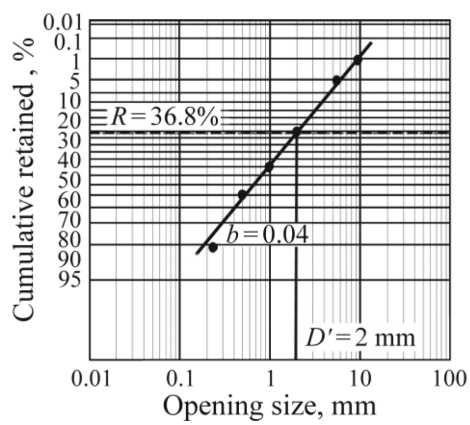

Fig. 3. The extraction of parameters D' and b from Rosin–Rammler graph for Lockhart limestone rock sample (plotted as per [11]).

Table 4. Mean values of penetration rate PR and specific energy SE calculated from the operational parameters of drill machines measured in field studies

Project	Rock Type	PR, m/min	Borehole Diameter, m	Feed Force, KN	Torque, KNm	SE, MJ/m^3
NJHPP	Murree Sandstone	0.43	0.05	2.03	0.06	185.08
GCL	Sakesar Limestone	0.51	0.11	8.99	0.52	107.43
KHPP	Granitic Gneiss	0.61	0.03	0.71	0.01	36.53
KCCL	Dolomite	0.77	0.08	3.11	0.12	30.70
KCCL	Lockhart Limestone	0.75	0.08	3.11	0.12	32.51
DGKCCL	Dungan Limestone	0.83	0.12	10.76	0.67	38.92
KHPP	Graphitic Gneiss	0.98	0.03	0.71	0.01	24.19
GHPP	Nagri Sandstone	1.05	0.07	3.37	0.13	23.58
MLCFL	Namal Limestone	1.14	0.09	4.26	0.19	20.16

1.2.2. Unconfined compressive strength (ucs) tests

The UCS tests were conducted on trimmed cylindrical rock samples, which had a length to diameter ratio ranging from 2.0 to 2.5 in accordance with the testing procedure specified in ASTM D-7012 [40] standard.

1.2.3. Brazilian tensile strength (bts) tests

The BTS tests were performed according to the recommendations of ASTM D-3967 [41] standard. The prepared rock discs of NX size had a height to diameter ratio of approximately 0.5 and were compressed diametrically until failure.

1.2.4. Point load strength (PLS) tests

The PLS tests were performed on core samples according to the testing procedures given by ASTM D-5731 [42] standard. These tests were conducted by loading rock cores in diametric orientations between conical platens of the machine. The length to diameter ratio was kept in the range of 1 to 1.5. The load was gradually increased until failure occurred within 10 to 60 s.

1.2.5. Schmidt rebound hardness (SRH) tests

The SRH tests were conducted on cylindrical rock samples by using *N*-type digital Schmidt rebound hammer having impact energy of 2.207 Nm. The measurements were taken in accordance with the ASTM D-873 [43] suggested method. Later the average of ten highest rebound number values measured using *N*-type device were converted to *L*-type Schmidt rebound number values by employing equation proposed by Aydin [44].

Table 5. Laboratory experimental results of nine rock units encountered at selected project sites

Rock Type	CI	D', mm	UCS	BTS	PLS	SRH	B_3	B_4	N, %	ρ, g/cm^3	V_p, km/s
			MPa								
Murree Sandstone	277	1.02	125	11.50	5.50	48.0	718.75	26.81	1.81	2.64	4.49
Sakesar Limestone	415	2.86	94	8.50	4.41	46.2	399.50	19.99	1.31	2.67	5.19
Granitic Gneiss	244	0.66	70	7.70	3.30	44.2	269.50	16.42	5.76	2.00	4.10
Dolomite	313	1.40	66	6.75	3.00	38.3	222.75	14.92	5.42	2.60	5.84
Lockhart Limestone	350	1.65	66	7.10	3.20	40.0	234.30	15.31	9.33	2.67	6.24
Dungan Limestone	373	2.12	60	7.16	3.17	38.9	214.80	14.66	33.06	2.58	5.70
Graphitic Gneiss	259	0.52	54	5.97	2.89	37.0	161.19	12.70	20.00	3.00	3.30
Nagri Sandstone	303	1.40	47	4.00	2.00	33.0	94.00	9.70	25.78	2.63	3.78
Namal Limestone	402	2.12	33	3.50	1.50	30.0	57.75	7.60	30.00	2.50	5.60

$B_3 = (\text{UCS}\times\text{BTS})/2$, $B_4 = \sqrt{B_3}$ —brittleness indices

Table 6. Regression models developed for the prediction of PR and SE from physico-mechanical rock properties

Penetration Rate, m/min	R^2	Specific Energy, MJ/m^3	R^2
PR = –0.008UCS + 1.348	0.86	SE = 1.923UCS – 75.945	0.88
PR = –0.096BTS + 1.447	0.89	SE = 19.871BTS – 81.831	0.73
PR = –0.191PLS + 1.397	0.87	SE = 42.085PLS – 80.011	0.81
PR = –0.040SRH + 2.380	0.97	SE = 7.176SRH – 228.124	0.59
PR = $-0.001B_3 + 1.067$	0.77	SE = $0.270B_3 - 15.738$	0.93
PR = $-0.041B_4 + 1.406$	0.89	SE = $8.932B_4 - 81.613$	0.83
PR = $0.016n + 0.544$	0.71	SE = $-2.541n + 92.851$	0.33

1.2.6. P-wave velocity

Primary wave velocities V_p were measured by using a digital Portable Ultrasonic Non-destructive Indication Tester (PUNDIT) in the laboratory as per ISRM [45] suggested method. PUNDIT transducers were positioned at both trimmed ends of the NX size rock cores of sufficient lengths. Then *P*-wave velocities were computed by measuring the time of propagation of sonic pulses through the specimens.

1.2.7. Density and porosity tests

The natural density of included rock units was computed by determining the weight and volume of prepared core specimens. A weighing balance of least count 0.01 g was used to determine the weight of rock specimen and the sample volume was calculated from average values of length and diameter of rock core measured with the help of a digital calliper. The porosity of rock samples was determined by using the saturation and caliper technique of the ISRM suggested methods [46] valid for the rock samples of regular dimensions.

2. TEST RESULTS AND DISCUSSION

Table 4 lists the values of penetration rate PR and specific energy SE computed by utilizing the data pertaining to operational parameters of drill machines recorded directly from drilling sites, whereas complete results obtained from laboratory testing including coarseness index CI, Rosin–Rammler absolute size constant D', physico-mechanical rock properties and brittleness indices are presented in Tab. 5. The test results of UCS and BTS were further used for the calculations of rock brittleness indices including B_3 and B_4 for each rock type. In this study the discussion of results is primarily focused on establishing relationships of PR and SE with rock properties as well as correlations of PR and bit diameter with CI and D'. Moreover, the validation of developed correlations (i.e. PR and SE versus rock properties) by employing statistical techniques (*F*-test and *t*-test) is also discussed.

Table 7. Validation of regression models developed for the prediction of PR from physico-mechanical rock properties

Geomechanical property	R^2	F_{model}	$F_{critical}$	*P*-value	$t_{calculated}$	t_{table}
UCS	0.86	41.31	5.32	0.000	–6.43	1.86
BTS	0.89	58.24	5.32	0.000	–7.63	1.86
PLS	0.87	47.04	5.32	0.000	–6.86	1.86
SRH	0.97	248.35	5.32	0.000	–15.76	1.86
B_3	0.77	24.02	5.32	0.002	–4.90	1.86
B_4	0.89	56.31	5.32	0.000	–7.50	1.86
n	0.71	16.75	5.32	0.005	4.09	1.86

2.1. Relationship of PR and SE with Physico-Mechanical Rock Properties

Relationships of PR and SE with mechanical and physical rock properties for all nine rock units are shown in Fig. 4. The figure depicts that there are significant correlations of both PR and SE with the UCS, BTS, PLS, SRH, B_3, B_4 and n. As expected the PR decreased linearly with increasing strength (UCS, BTS, PLS), hardness (SRH) and brittleness (B_3 and B_4) values of the included rock units, while an upward linear trend was observed between PR and rock porosity values. Similar relationships of penetration rate with engineering properties of rocks have also been proposed by numerous past researchers [17, 20, 21, 47]. On the other hand strong positive linear relationships of SE of drilling with UCS, BTS, PLS, SRH, B_3, B_4 were found. However, the specific energy dropped linearly with corresponding rise in rock porosity n and a weak correlation can be observed. The correlations of SE of drilling with physico-mechanical rock properties developed in earlier investigations also closely coincide with the correlations established in this study [25, 48–51].

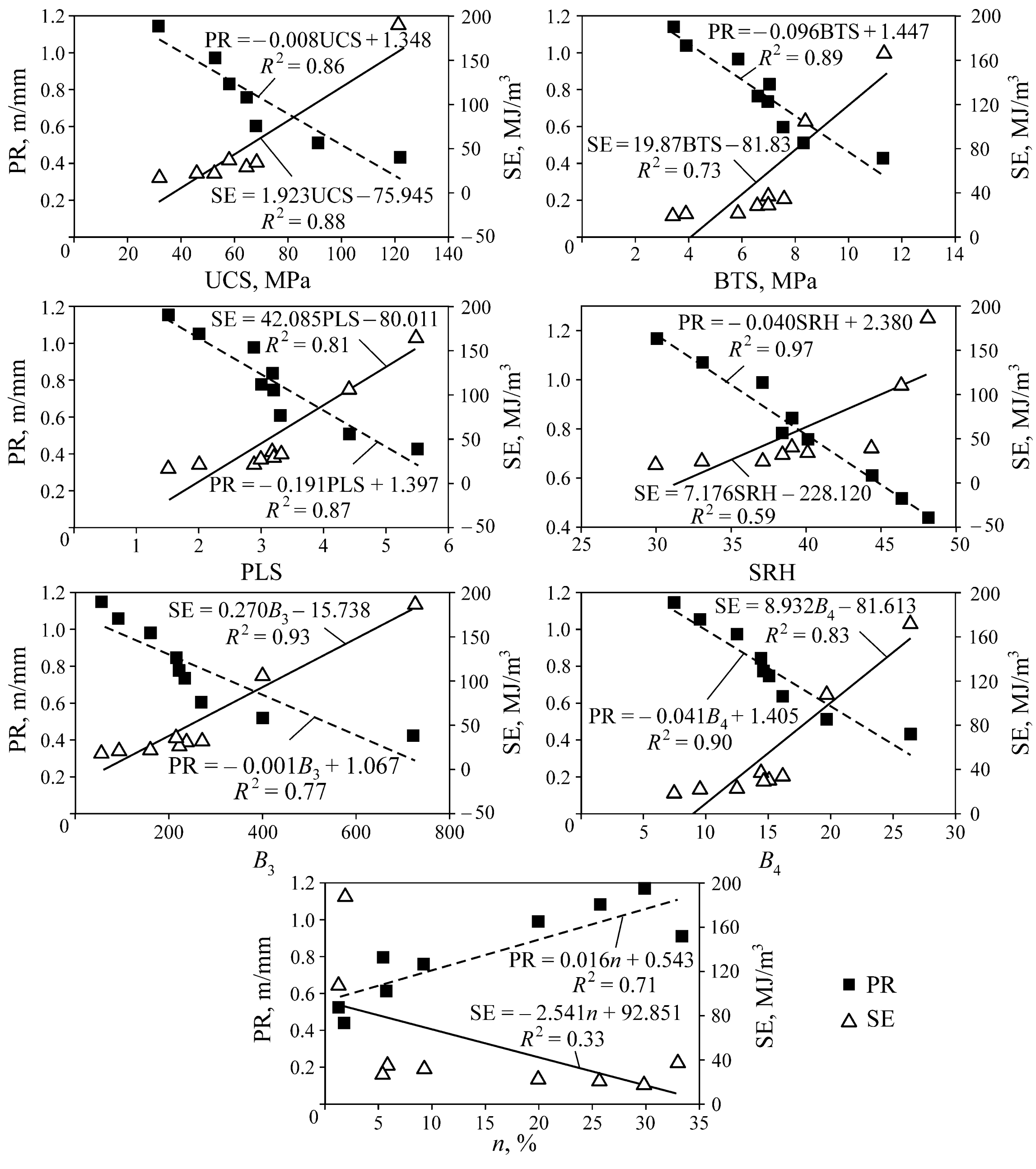

Fig. 4. Linear correlations of penetration rate with coarseness index and Absolute size constant of nine selected rock.

Table 8. Validation of regression models developed for the prediction of SE from physico-mechanical rock properties

Geomechanical property	R^2	F_{model}	$F_{critical}$	P-value	$t_{calculated}$	t_{table}
UCS	0.88	53.46	5.32	0.000	7.31	1.86
BTS	0.73	18.93	5.32	0.003	4.35	1.86
PLS	0.81	30.08	5.32	0.001	5.48	1.86
SRH	0.59	9.99	5.32	0.016	3.16	1.86
B_3	0.93	91.41	5.32	0.000	9.56	1.86
B_4	0.83	33.14	5.32	0.001	5.76	1.86

Using the relationships of PR and SE plotted against mechanical and physical rock properties the prediction models were developed (Tab. 7) for the estimation of PR and SE. In the case of PR the models based on SRH, B_4, BTS, UCS, PLS and BTS showed better prediction performance as compared to the models developed with B_3 and porosity. Similarly, in the case of SE the models based on rock parameters including B_3, B_4, UCS and PLS depict better forecasting ability, than the other relationships. To validate the significance of proposed correlations of PR and SE with rock properties (Tab. 6), F-test and t-test statistics were adopted by using SPSS-21 statistical software pack for windows.

Table 7, 8 present the computed and tabulated F-test values along with corresponding P-values at the 95% level of significance ($\alpha = 0.05$) for the proposed prediction models (PR and SE versus geomechanical rock properties). As can be seen that F_{model} values are greater than $F_{critical}$ values at predefined significance level showing the correctness of the models. It may also be noted that the P-values of the independent variables (UCS, BTS, PLS, SRH, B_3, B_4 and n) are less than the value of α indicating their significance. Similarly at 95% confidence level the calculated t scores are greater than the tabulated t scores in both Tables 7, 8 and hence showing that the proposed models are valid statistically.

Table 9. Proposed regression models of PR with CI and D'

Rock Unit	PR versus CI	R^2	PR versus D'	R^2
Murree Sandstone	PR = 0.004CI – 0.698	0.94	PR = 0.199D' + 0.226	0.86
Sakesar Limestone	PR = 0.003CI – 0.776	0.87	PR = 0.118D' + 0.172	0.90
Granitic Genesis	PR = 0.006CI – 0.778	0.89	PR = 0.436D' + 0.319	0.87
Dolomite	PR = 0.004CI – 0.420	0.91	PR = 0.252D' + 0.437	0.90
Lockhart Limestone	PR = 0.001CI + 0.335	0.91	PR = 0.094D' + 0.598	0.87
Dungan Limestone	PR = 0.009CI – 2.337	0.94	PR = 0.283D' + 0.301	0.79
Graphitic Gneiss	PR = 0.005CI – 0.198	0.96	PR = 0.428D' + 0.757	0.90
Nagri Sandstone	PR = 0.002CI + 0.527	0.88	PR = 0.109D' + 0.895	0.90
Nammal Limestone	PR = 0.005CI – 0.843	0.91	PR = 0.236D' + 0.541	0.85

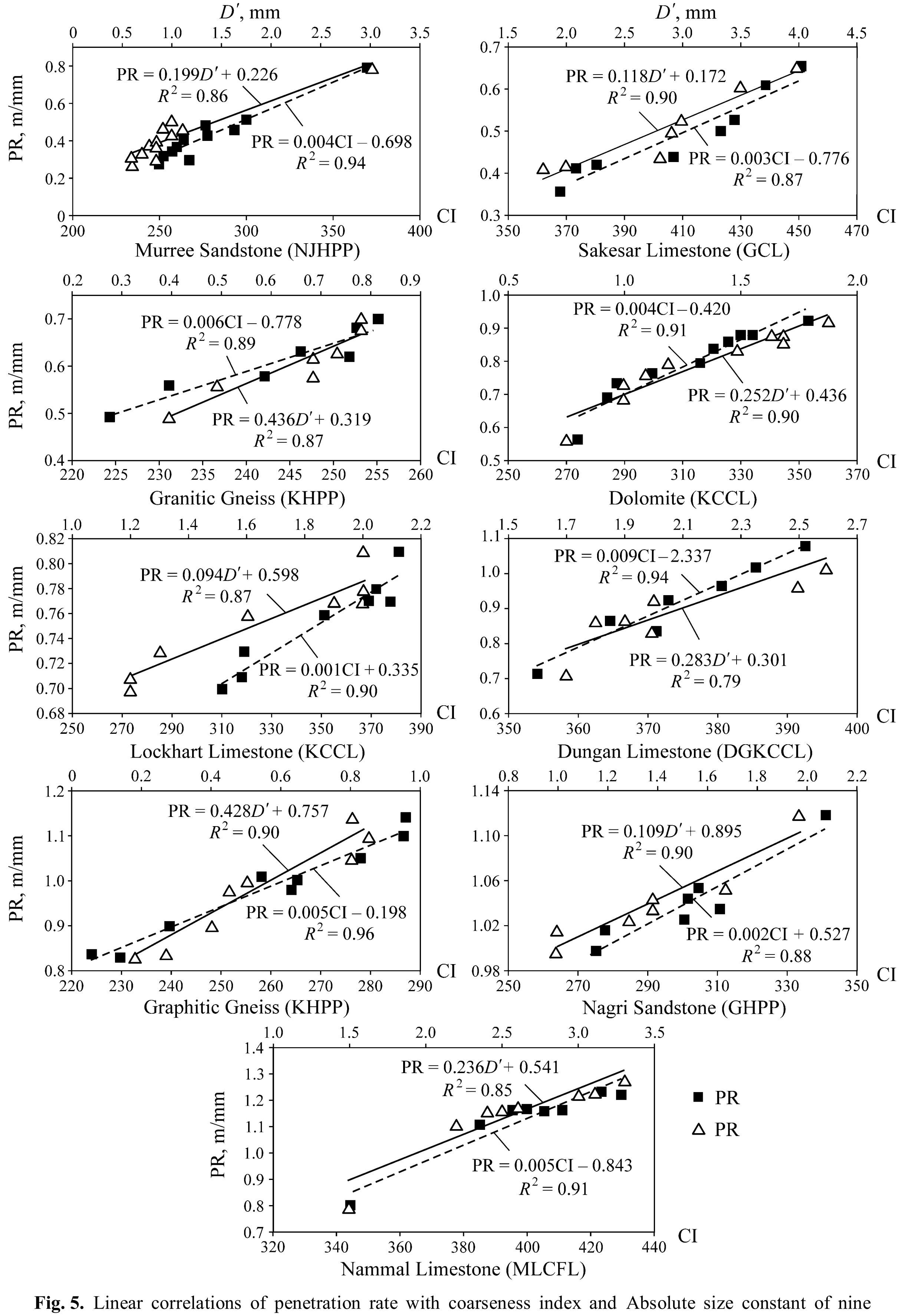

Fig. 5. Linear correlations of penetration rate with coarseness index and Absolute size constant of nine selected rock.

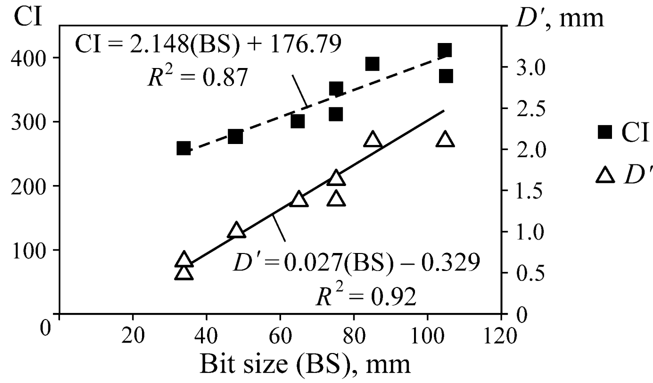

Fig. 6. Correlations of CI and D' with bit size.

2.1. Relationship of PR with CI and D'

In this study efforts have also been made to correlate the CI and D' values with the corresponding rock penetration rates measured at the each selected drilling location. For each rock unit the plots of penetration rate PR as a function of CI and D' are presented in Fig. 5. In general strong positive linear correlations of penetration rates with respective CI and D' values can be observed. The models so developed (Table 9) can be utilized for the prediction of penetration rate PR of button bits employed rotary-percussive drills from coarseness index CI and the absolute size constant D' particularly in the selected rock units. Altindag [52] proposed equations for the estimation of PR from CI and mean particle size values for limestone rock only. Similarly, Altindag [7] in a research work developed both linear as well as exponential relationships of PR with coarseness index and mean particle size based on the drillability data gathered from limestone and marl quarries. The linear correlations generally match with the relations established in this study. Kahraman et al. [8] in their research work also proposed relationships between penetration rates and CI values and penetration rates and median particle size MPS values.

2.3. Effect of Drill Bit Size on CI and D'

It can be seen that CI and D' show linearly increasing trends (Fig. 6) with the bit diameter; meaning as the bit size increases coarseness index and mean particle size also increases. In the case of CI versus bit diameter similar trend was found by Bullock [27] while working on two hydraulic drills. The cited author concluded that chip size of rock increased linearly with bit size up to a certain diameter and further increase in the bit diameter resulted in decrease in chip size mainly due to type of drill (top hammer drill or DTH) and geological discontinuities (joint sets, bedding planes, foliations etc.).

The prediction of penetration rate and specific energy of drilling are frequently required in mining and tunneling projects. Both PR and SE are partly dependent on rock properties (mechanical and physical properties) and partly on the operational parameters of drill machine. This study includes recording of penetration rates and measurement of SE of rotary percussive drills from seven ongoing excavation projects of Pakistan, covering a total of nine different rock units. Sieve analysis of collected drill cuttings was performed to calculate the coarseness index and the mean particle size values. Rock mechanics testing was conducted to determine the physico-mechanical properties and brittleness indices (B_3 and B_4) of included rock units.

CONCLUSIONS

It was concluded that UCS, BTS, PLS, SRH, B_3, B_4 significantly dominate the penetration rate and specific energy of rotary percussive drills. Rock porosity however, exhibited good relationship with PR but, it showed a weak correlation with SE of drilling. Amongst the physico-mechanical rock properties tests included in this research PLS and SRH tests can easily be conducted in the field and hence can be utilized for the quick assessment of PR and SE from the proposed correlations. Meaningful positive linear correlations of penetration rate with coarseness index CI and absolute size constant D' were established for each rock unit included in this work. The higher values of coarseness index and mean particle size represent higher drillability values. It explains that most of the available energy for drilling was consumed in rock breakage at the tool rock interface. Strong linear correlations between bit diameter and CI and D' were also proposed. Future studies could be directed to examine the influence of other rock parameters like petrography, the orientation and the strength of weakness planes in predicting the penetration rate and specific energy of drilling from physico-mechanical properties, CI and D'.

REFERENCES

1. McFeat-Smith, I., and Fowell, R.J., Selection and Application of Roadheaders for Rock Tunneling, *Proc. Rapid Excavation and Tunneling Conference–RETC*, Altanta, 1979.
2. Tanaino, A.S., Rock Classification by Drillability. Part I: Analysis of the Available Classifications, *J. Min. Sci*., 2005, vol. 41, no. 6, pp. 541–549.
3. Altindag, R., Correlation of Specific Energy with Rock Brittleness Concepts on Rock Cutting, *J. South Afr. Inst. Min. Metall*., 2003, vol. 103, no. 3, pp. 163–172.
4. Pfleider, E.P., and Blake, R.L., Research on the Cutting Action of the Diamond Drill Bit, *Min. Eng*., 1953, vol. 5, pp. 187–195.
5. Rabia, H., and Brook, N., An Empirical Equation for Drill Performance Prediction*, Proc. 21st Symp. on Rock Mech*., University of Missouri-Rolla, USA, 1980, pp. 104–112.
6. Ersoy, A., and Waller, M.D., Drilling Detritus and the Operating Parameters of Thermally Stable PDC Core Bits, *Int. J. Rock Mech. Min. Sci*., 1997, vol. 34, no. 7, pp. 1109–1123.
7. Altindag, R., Evaluation of Drill Cuttings in Prediction of Penetration Rate by Using Coarseness Index and Mean Particle Size in Percussive Drilling, *Geotech. and Geol. Eng*., 2004, vol. 22, pp. 417–425.
8. Kahraman, S., Develi, K., and Yasar, E., Predicting the Penetration Rate of Percussive Blast Hole Drills Using Coarseness Index and Median Particle Size, *CIM Bulletin*, 2004, vol. 97, no. 15, pp. 1–4.
9. Tuncdemir, H., Bilgin, N., Copur, H., and Balci, C., Control of Rock Cutting Efficiency by Muck Size, *Int. J. Rock Mech. Min. Sci*., 2008, vol. 45, pp. 278–288.
10. Abu Bakar, M.Z., and Gertsch, L.S., Radial Pick Cutting Performance in Dry and Saturated Sandstone, Society for Mining, *Metallurgy and Exploration*, 2012, vol. 332, pp. 396–405.
11. Abu Bakar, M.Z., Gertsch, L.S., and Rostami, J., Evaluation of Fragments from Disc Cutting of Dry and Saturated Sandstone, *Rock Mech. Rock Eng*., 2014, vol. 47, pp. 1891–1903.
12. Selmer-Olsen, R., and Blindheim, O.T., On the Drillability of Rock by Percussive Drilling, *Proceedings of the 2nd Congress of the Int. Society for Rock Mechanics*, Belgrade, Yugoslavia, 1970, pp. 65–70.
13. Howarth, D.F., Adamson, W.R., and Berndt, J.R., Correlation of Model Tunnel Boring and Drilling Machine Performances with Rock Properties, *Int. J. Rock Mech. Min. Sci*., 1986, vol. 23, pp. 171–175.
14. Thuro, K., and Spaun, G., Introducing the Destruction Work as a New Rock Property of Toughness Referring to Drillability in Conventional Drill and Blast Tunneling, Barla, G. (Ed.*), Eurock 96: Prediction and Performance in Rock Mech. and Rock Eng.*, 1996, vol. 2, pp. 707–713.
15. Thuro, K., Drillability Prediction: Geological Influences in Hard Rock Drill and Blast Tunneling, *Geol. Rundsch*., 1997, vol. 86, pp. 426–438.

16. Altindag, R., The Evaluation of Rock Brittleness Concept on Rotary Blast Hole Drills, *J. South Afr. Inst. Min. Metall*., 2002, vol. 102, pp. 61–66.
17. Kahraman, S., Bilgin N., and Feridunoglu, C., Dominant Rock Properties Affecting the Penetration Rate of Percussive Drills, Int. J. Rock Mech. Min. Sci., 2003, vol. 40, pp. 711–723.
18. Dahl, F., Bruland, A., Jakobsen, P.D., Nilsen, B., and Grøv, E., Classifications of Properties Influencing the Drillability of Rocks, Based on the NTNU/SINTEF Test Method, *Tunneling and Underground Space Technology*, 2012, vol. 28, pp. 150–158.
19. Seifabad, M.C., and Ehteshami, P., Estimating the Drilling Rate in Ahvaz Oil Field, *J. Petrol. Exploration Prod. Technology*, 2013, vol. 3, pp. 169–173.
20. Ngerebara, O.D., and Youdeowei, P., Correlation of Mechanical Properties of Some Rocks in South-Eastern Nigeria, *Int. J. Sci. and Res. Pub*., 2014, vol. 4, pp. 1–6.
21. Hoseinie, S.H., Ataei, M., and Aghababaie, A., A laboratory Study of Rock Properties Affecting the Penetration Rate of Pneumatic Top Hammer Drills, *J. Min. and Env*., 2014, vol. 5, pp. 25–34.
22. Protodyakonov, M.M., Mechanical Properties and Drillability of Rocks*, Proceedings of the 5th Symp. on Rock Mech*., University of Minnesota, 1962, pp. 103–118.
23. Teale, R., The Concept of Specific Energy in Rock Drilling, *Rock Mech. Min. Sci*., 1964, vol. 2, pp. 57–73.
24. Mellor, M., Normalization of Specific Energy Values, *Int. J. Rock Mech. Min. Sci*., 1972, vol. 9, pp. 661–663.
25. Copur, H., Tuncdemir, H., Bilgin, N., and Dincer, T., Specific Energy as a Criterion for the Use of Rapid Excavation Systems in Turkish Mines, *Trans. Int. Min. Metall. Sect. Min. Tech*., 2001, vol. 110, pp. A149–A157.
26. Rabia, H., Specific Energy as a Criterion for Drill Performance Prediction, *Int. J. Rock Mech. Min. Sci. Geomech*., 1982, vol. 19, pp. 39–42.
27. Bullock, R.L., Tunneling and Underground Construction Techniques, *Mining 383 Course*, Missouri University of Science and Technology, Rolla, MO, USA, 2009.
28. Roxborough, F.F., Research in Mechanical Rock Excavation: Progress and Prospects, *Proceedings of the Rapid Excavation and Tunneling Conference*, 1985, vol. 1, pp. 225–243.
29. Fowell, R.J., The Mechanics of Rock Cutting, Hudson, J.A. (Eds.), *Comprehensive Rock Engineering*, 1993, vol. 4, pp. 155–175.
30. Evans, I., A Theory on the Basic Mechanics of Coal Ploughing, *Proceedings of the Int. Symp. on Min. Research*, Missouri, 1961, vol. 2, pp. 761–798.
31. Nishimatsu, Y., The Mechanics of Rock Cutting, Int. J. Rock Mech. Min. Sci., 1972, vol. 9, pp. 261–270.
32. Atici, U., and Ersoy, A., Correlation of Specific Energy of Cutting Saws and Drilling Bits with Rock Brittleness and Destruction Energy, *J. of Materials Proc. Tech*., 2008, vol. 209, pp. 2602–2612.
33. Paone, J., Madson, D., and Bruce, W.E., Drillability Studies—Laboratory Percussive Drilling, *USBM RI 7300*, 1969.
34. Moore, P.L., *Drilling Practices Manual*, Tulsa: Penn Well Books, 1974.
35. Huang, S.L., and Wang, Z.W., The Mechanics of Diamond Core Drilling of Rocks, *Int. J. Rock Mech. Min. Sci. Geomech. Abst*., 1997, vol. 34, pp. 6–12.
36. ASTM D4543, Standard Practices for Preparing Rock Core as Cylindrical Test Specimens and Verifying Conformance to Dimensional and Shape Tolerances, 2008.
37. Roxborough, F.F., and Rispin, A., The Mechanical Cutting Characteristics of the Lower Chalk, *Tunnels and Tunneling*, 1973, pp. 45–67.
38. Rosin, P., and Rammler, B., The Laws Governing the Fineness of Powdered Coal, *J. Inst Fuel*, 1933, vol. 7, pp. 29–36.
39. Aytekin, Y., The Measurement Methods of Fine Particle, *Ege. Univ. Press*., no. 2, 1979, pp. 114.

40. ASTM D7012, Standard Test Method for Compressive Strength and Elastic Moduli of Intact Rock Core Specimens under Varying States of Stress and Temperatures, 2010.
41. ASTM D3967, Standard Test Method for Splitting Tensile Strength of Intact Rock Core Specimens, ASTM International, West Conshohocken, PA, 2016. doi.org/10.1520/D3967-16.
42. ASTM D573, Standard Test Method for Determination of the Point Load Strength Index of Rock and Application to Rock Strength Classification, 2008.
43. ASTM D83, Standard Test Method for Determination of Rock Hardness by Rebound Hammer Method, 2005.
44. Aydin, A., ISRM Suggested Method for Determination of the Schmidt Hammer Rebound Hardness: Revised version, *Int. J. Rock Mech. Min. Sci*., 2009, vol. 46, no. 3, pp. 627–634.
45. ISRM, Suggested Methods for Determining Sound Velocity, *Int. J. of Rocks Mech. and Min. Sci. and Geomech*., 1978, vol. 15, pp. 53–58.
46. ISRM, Suggested Methods for Determining Water Content, Porosity, Density, Absorption and Related Properties and Swelling and Slake-Durability Index Properties, *Int. J. of Rocks Mech. and Min. Sci. and Geomech*., 1979, vol. 16, pp. 141–156.
47. Bilgin, N., and Kahraman, N., Drillability Prediction in Rotary Blast Hole Drilling, *1st Int. Min. Congress and Exhibition of Turkey-IMCET*, 2003.
48. Roxborough, F.F., and Sen, G.C., Breaking Coal and Rock, *Australasian Coal Mining Practice*, 1986, vol. 12, pp. 130–147.
49. Bilgin, N., Seyrek, T., and Sahriar, K., Roadheader Performance in Istanbul, Golden Horn Clean up Contributes Valuable Data, *Tunnels and Tunneling*, 1988, vol. 20, no. 6, pp. 41–47.
50. Reddish, D.J., and Yasar, E., A New Portable Rock Strength Index Test Based on Specific Energy of Drilling, *Int. J. of Rock Mech. Min. Sci. and Geomech*., 1996, vol. 33, no. 5, pp. 543–548.
51. Tiryaki, B., and Dikmen, A.C., Effects of Rock Properties on Specific Cutting Energy in Linear Cutting of Sandstones by Picks, *Rock Mech. and Rock Eng*., 2006, vol. 39, no. 2, pp. 89–120.
52. Altindag R. Estimation of Penetration Rate in Percussive Drilling by Means of Coarseness Index and Mean Particle Size, *Rock Mech. and Rock Eng*., 2003, vol. 36, no. 4, pp. 323–332.